

Closed-Loop Transmit Diversity Techniques for Small Wireless Terminals and Their Performance Assessment in a Flat Fading Channel

Raqibul Mostafa, Ramesh C. Pallat, Uwe Ringel, Ashok A. Tikku, and Jeffrey H. Reed

Closed-loop transmit diversity is considered an important technique for improving the link budget in the third generation and future wireless communication standards. This paper proposes several transmit diversity algorithms suitable for small wireless terminals and presents performance assessment in terms of average signal-to-noise ratio (SNR) and outage improvement, convergence, and complexity of operations. The algorithms presented herein are verified using data from measured indoor channels with variable antenna spacing and the results explained using measured radiation patterns for a two-element array. It is shown that for a two-element array, the best among the proposed techniques provides SNR improvement of about 3 dB in a tightly spaced array (inter-element spacing of 0.1 wavelength at 2 GHz) typical of small wireless devices. Additionally, these techniques are shown to perform significantly better than a single antenna device in an indoor channel considering realistic values of latency and propagation errors.

Keywords: Transmit diversity, handset, wireless channel.

Manuscript received June 29, 2011; revised Oct. 4, 2011; accepted Nov. 10, 2011

This work was supported by the Texas Instrument and the Office of Naval Research NAVCIITI program.

Raqibul Mostafa (phone: +88 2 9125912, mmostafa@eee.uui.ac.bd) is with the Electrical Electronics Engineering Department, United International University, Dhaka, Bangladesh.

Ramesh C. Pallat (rchembil@qualcomm.com) is with Qualcomm Inc., New Jersey, USA.

Uwe Ringel (fringel@ifn.etu-dresden.de) is with Siemens, Germany.

Ashok A. Tikku (aat2119@columbia.edu) is with Columbia University, NY, USA.

Jeffrey H. Reed (reedjh@vt.edu) is with the Department of Electrical and Computer Engineering, Virginia Tech, Blacksburg, VA, USA.

<http://dx.doi.org/10.4218/etrij.12.0111.0413>

I. Introduction

Antenna arrays find applications in wireless communications systems for their capabilities in countering fading, mitigating multipath distortion, and improving signal-to-noise ratio (SNR). Antenna arrays are predominantly used in the receive mode; however, there has been an increased interest in using antenna arrays in the transmit mode. Transmit diversity provides essentially the same benefits as receive diversity and can also be extended to perform transmit-beamforming [1]-[6].

Traditionally, closed-loop transmit-diversity techniques have been studied for implementation at the base station. The W-CDMA standard has provisions for feedback information to implement closed-loop transmit diversity [7] that can support High-Speed Downlink Packet Access [8]. As reported in [9]-[12], transmit diversity techniques that employ feedback do not address the effect of non-idealities such as channel estimation errors, feedback delay, quantization, and feedback errors that are likely to be present in a practical system. The effect of propagation delay on the performance of a closed-loop transmit diversity system in the absence of other non-idealities is addressed in [13], [14]. Reduction of feedback payload has been considered under the assumption of perfect channel knowledge in [15], [16]. The effect of feedback errors has been studied through simulation and analysis in [17]-[19]. Analysis of the impact of channel estimation errors on the performance of transmit diversity with feedback is presented in [20], [21].

With the advent of fast and low-power processing platforms as well as the miniaturization of RF components, array processing will become feasible in small wireless terminals.

Performance improvements reported in [22] on receive diversity techniques applied over channel measurement results show the efficacy of using multiple antennas at the handsets. Moreover, there is an emerging commercial interest in handsets with antenna array [23]. However, transmit diversity applied at the small terminals is a topic that has not been explored much. Theoretical investigations in [24], [25] as well as practical implementations in [26] have shown that transmit diversity on the mobile device side can significantly improve the reverse link performance. However, the implementation aspects, which include channel estimation process, impact of weight vector convergence, and the effect of envelope cross correlation at the mobile terminal, have not been addressed. Hence, in this paper, we examine the effect of the above factors along with other non-idealities when transmit diversity techniques are applied to a mobile terminal. It should be pointed out that transmit diversity techniques applied to existing high-speed wireless standards focus on multiple-input multiple-output (MIMO) configuration having antenna arrays at both the transmitter and the receiver with an objective of increasing the data rate over that which is achievable from a single antenna system. However, those techniques rely on four antenna elements [27], require additional processing (for example, higher order modulation and pilot interference cancellation) to realize the full potential [28], and tend to be complex in nature and thus may not be well suited for small wireless terminals.

This paper is organized as follows: Section III introduces proposed algorithms, section IV presents simulation results for performance evaluation of the proposed techniques, and section V provides the conclusion.

II. Background

In this paper, we first present a study of simple closed-loop transmit diversity techniques that are suitable for small mobile wireless devices under practical operating conditions. A model representing a closed-loop transmit diversity system along with the constraints of feedback errors, propagation delays, and quantization is shown in Fig. 1.

Considering the stated operating constraints, the major design criteria of transmit diversity algorithms for mobile devices should be simplicity and rapid convergence. The first condition is necessary to avoid using up computational resources and conserving power while the second condition is vital for reliable operation in time-varying channels. In light of this, the proposed transmit diversity scheme is based on using a simple weight vector without any additional temporal encoding. For a closed-loop transmit diversity system, the receiver assists in channel estimation and feedback of these estimates to the transmitter. Thus, a reduced-complexity estimation and

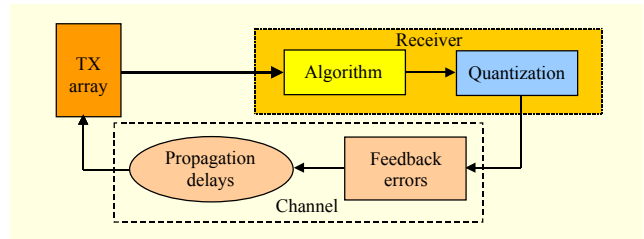


Fig. 1. Model representing closed-loop transmit diversity system under practical operating conditions.

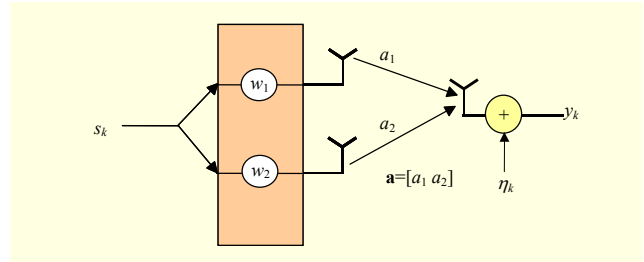


Fig. 2. Block diagram for implementation of transmit diversity.

feedback process at the receiver along with simple processing at the transmitter will reduce consumption of system resources and result in an efficient communication system. Such a reduced complexity implementation will be valuable for ad-hoc communication between mobile devices and also in sensor networks (for example, in a highly loaded cellular system [that is, a system with a large number of active users]). We address relevant practical performance issues for small wireless terminals, which include: assessment of convergence characteristics, improvement in mean SNR and outage probability under imperfect channel knowledge, and implementation issues related to latency, quantization, and feedback errors. Additionally, we present indoor vector channel measurements for antenna arrays with different inter-element spacing that are relevant to a handset form factor. We show that transmit diversity at handsets even with tightly spaced array show better performance than in a single antenna case. Because of the tight spacing between the elements, the effect of mutual coupling (which is usually neglected in base station applications and other simulation-based studies) becomes an important factor. This is discussed in our results with vector channel measurements to provide valuable insights on the effect of mutual coupling. To the best of our knowledge, no published results exist for field measurement-based performance of closed-loop transmit diversity at the handsets.

III. Algorithm Development

Figure 2 shows a schematic diagram of a transmit diversity implementation with an antenna array of two elements and a

single antenna receiver. The channel vector \mathbf{a} (row vector) consists of individual complex channel gains a_i , from the i -th element to the receiver. The information symbols at the transmitter are scaled by the complex weight vector \mathbf{w} (column vector). The output at the receiver is given by,

$$y_k = \mathbf{a}\mathbf{w}s_k + \eta_k = Gs_k + \eta_k, \quad (1)$$

where s_k is the k -th transmitted symbol, η_k is the k -th noise sample at the receiver, and G is the gain observed at the receiver. The weight vector is chosen such that the SNR is maximized at the receiver while maintaining a constant transmit power. Mathematically,

$$\begin{aligned} & \max (\mathbf{w}^* \mathbf{a}^* \mathbf{a} \mathbf{w}) \gamma_0, \\ & \text{s.t. } \mathbf{w}^* \mathbf{w} = 1, \end{aligned} \quad (2)$$

where “*” corresponds to the Hermitian transpose operation, γ_0 is the SNR for a single antenna in an additive white Gaussian noise (AWGN) channel, and the total transmit power is arbitrarily set to unity. Recognizing this eigenvalue problem, the optimal solution is known as

$$\mathbf{w}_{\text{opt}} = \frac{\mathbf{a}^*}{\|\mathbf{a}\|_2}. \quad (3)$$

Here, $\|\cdot\|_2$ refers to the norm-2 of a vector. In a closed-loop transmit diversity system, the channel can be estimated at the receiver and made available to the transmitter through feedback. While (3) provides maximal ratio transmission (MRT) or the optimal solution, a suboptimal solution is also possible, known as equal gain transmission (EGT) based on co-phasing between the individual channel gains. The following subsections present the proposed algorithms under these two categories of solutions.

1. EGT Techniques

Principle: The EGT solution for the weight vector is of the form $\mathbf{w} = \frac{1}{\sqrt{2}} [1 \ e^{-j\hat{\beta}}]^T$, where $\hat{\beta}$ is an estimate of the phase difference between the individual channel gains. The estimation process is based on employing a phase search technique using feedback from the receiver. Two new search algorithms have been proposed in this paper: the bisection method and the early-late method. These techniques differ from the equal gain approach presented in [10] in that they form an estimate of β without the assumption of perfect channel knowledge.

A. Bisection Method

Description: This is an iterative method that starts with a value of $\beta_0 \in [0, 2\pi]$. At any iteration index k , three successive

symbols are transmitted with three different phase values for the weight vector: $\beta_a = \beta_0$, $\beta_b = \beta_0 + 2^{-k}\pi$, and $\beta_c = \beta_0 - 2^{-k}\pi$. The receiver identifies the index of the symbol that is associated with the maximum signal strength and feeds this index back to the transmitter. For the next iteration and transmission, the transmitter updates the current phase (β_a) with this feedback and computes the other two phase values (β_b and β_c). The process continues until further phase adjustments yield negligible changes in phase values.

Challenges: The convergence process is impacted by the quality of the estimate of the received signal power. A high operating SNR provides better channel estimates and, consequently, a satisfactory performance of the bisection technique. Otherwise, the power estimates are less accurate and the technique may get stuck in a local maxima. This problem may be alleviated by averaging a number of symbols for each phase adjustment. Simulation results indicate that a total of about five iterations (or fifteen symbols) is usually sufficient to achieve convergence.

B. Early-Late Technique

Description: The search for an optimal β can be carried out by a gradient-based search where the transmitter successively transmits two symbols with two different β_1 and β_2 . The approach borrows from the traditional early-late gate symbol synchronization technique [29]. After estimating the power for the two consecutive symbols, the gradient is formulated as

$$\nabla_{\beta} = \frac{|y_{\beta_1}|^2 - |y_{\beta_2}|^2}{-\Delta\beta}, \quad (4)$$

where y_{β_1} and y_{β_2} refers to the received signal corresponding to β_1 and β_2 , respectively, and $\Delta\beta = \beta_1 - \beta_2$. This information is relayed back to the transmitter that then updates β as

$$\begin{aligned} \beta_{1,\text{new}} &= \beta_1 + \mu \nabla_{\beta}; \beta_{2,\text{new}} = \beta_{1,\text{new}} + \Delta\beta \\ & \text{or} \end{aligned} \quad (5)$$

$$\beta_{2,\text{new}} = \beta_2 + \mu \nabla_{\beta}; \beta_{1,\text{new}} = \beta_{2,\text{new}} + \Delta\beta.$$

Here, $\Delta\beta$ and μ refer to angle step-size and update step-size, respectively. The transmitter then generates the weight vectors and transmits new symbols with these two weight vectors, and then the process is repeated. The algorithm is able to track channel dynamics without periodic initialization.

Challenges: The challenges for this algorithm are similar to those for the bisection method, and the convergence process is relatively slower.

2. MRT Techniques

Principle: The MRT principle has been applied for MIMO in [30] under the assumption of perfect channel state information

and feedback. We propose techniques that build on this principle and generate channel estimates in a block or recursive manner. The proposed techniques are based on least squares (LSs) or gradient estimate algorithms: the LS-based, the subspace-based, the least mean square-based (LMS), and the hybrid method.

A. LS

Description: This technique combines the LS principle and the weight perturbation method to estimate the vector channel in either supervised (training) or unsupervised (blind) mode. In the supervised mode, a sequence of training symbols transmitted with a predefined sequence of weight vectors assists the receiver in the estimation process. In the unsupervised mode, both the symbol sequence and the channel gains are estimated in a recursive manner via the alternating projection method.

Let \mathbf{s} be the training sequence containing N symbols, \mathbf{W} be the $2 \times N$ matrix containing N vectors of perturbed weights, and \mathbf{Y} be the diagonal matrix of N received samples in the supervised mode. The LS problem is formulated as

$$\mathbf{a} = \arg \min \|\mathbf{sY} - \mathbf{aW}\|_2^2, \quad (6)$$

and the solution for the channel estimate can be written as

$$\mathbf{a} = \mathbf{sYW}^* (\mathbf{WW}^*)^{-1}. \quad (7)$$

For the unsupervised or blind LS technique, one can formulate an iterative solution as

$$\mathbf{a}^{(i+1)} = \arg \min_{\mathbf{a}} \left(\sum_{k=1}^N (y_k - \mathbf{a} \mathbf{w}_k s_k^{(i)})^2 \right), \quad (8)$$

$$\mathbf{s}^{(i+1)} = \arg \min_{\mathbf{s}} \left(\sum_{k=1}^N (y_k - \mathbf{a}^{(i+1)} \mathbf{w}_k s_k)^2 \right), \quad (9)$$

where $\mathbf{a}^{(i)}$ and $\mathbf{s}^{(i)}$ denote the estimated channel vector and the symbol vector at the i -th iteration, respectively.

Challenges: The LS algorithm needs a satisfactory level of operating SNR for reliable operation and rapid convergence.

B. Subspace Method

Description: The projection of an arbitrary weight vector \mathbf{w}_0 onto the channel vector \mathbf{a}^H is given by [31]

$$\mathbf{v} = \frac{\mathbf{a}^* \mathbf{a}}{\mathbf{a} \mathbf{a}^*} \mathbf{w}_0. \quad (10)$$

Thus, the optimum weight vector \mathbf{w}_{opt} can be rewritten as a normalized version of \mathbf{v} . Defining the cost function as $J(\mathbf{w}) = (\mathbf{w}^* \mathbf{a} \mathbf{a}^* \mathbf{w}) \gamma_0$, the optimum weight vector can be expressed as the gradient of the cost of the function evaluated

at any arbitrary \mathbf{w}_0 ,

$$\mathbf{w}_{\text{opt}} = \frac{\nabla J(\mathbf{w}_0)}{\|\nabla J(\mathbf{w}_0)\|_2}. \quad (11)$$

Each derivative term in the gradient of the cost function can be estimated numerically; for example, the gradient with respect to the real part of w_1 or w_1^R is shown as

$$\frac{\partial J}{\partial w_1^R} \approx \frac{J \left(\begin{matrix} w_1^R + \Delta \\ w_2^R + jw_2^I \end{matrix} \right) - J \left(\begin{matrix} w_1^R + jw_1^I \\ w_2^R + jw_2^I \end{matrix} \right)}{\Delta}. \quad (12)$$

Challenges: The gradient estimate depends on the amount of perturbation Δ as well as the additive noise in the system. Δ should be large when the background noise is strong. Another observation is that four different weight perturbations are needed to estimate the gradient of the cost function for a two-element array. Since the estimate of each derivative term may require the transmission of multiple symbols, the total number of symbols required for this method can be high. However, an advantage of the subspace method is its unsupervised mode of operation.

C. LMS Algorithm

Description: The LMS is a stochastic gradient-based algorithm and as such requires an estimate of $\nabla J(\mathbf{w})$. With numerical estimation of the gradient as $\hat{\nabla} J(\mathbf{w})$, the recursive weight update equation can be expressed as

$$\begin{aligned} \mathbf{z}_k &= \mathbf{w}_k + \mu \hat{\nabla} J(\mathbf{w}_k), \\ \mathbf{w}_{k+1} &= \frac{\mathbf{z}_k}{\|\mathbf{z}_k\|_2}. \end{aligned} \quad (13)$$

Challenges: The stability and convergence rate for LMS-type algorithms depend on the step-size μ . In general, the step-size is chosen to be small to ensure stability and thus the LMS approach is slow. However, the LMS method can operate without the use of a dedicated training sequence.

D. Hybrid Method

Description: A hybrid method can be devised where the subspace method is used in the initial iterations, and then the LMS technique is used for final convergence. The direct estimate of \mathbf{w}_0 followed by fine tuning with the LMS combines good transient characteristics of the subspace method and the stable steady state performance of the LMS. Simulation results indicate that the switching can be within one or two iterations of the subspace algorithm. Periodic re-initialization will provide good tracking capability of the algorithm.

3. Evaluation of Complexity of Proposed Algorithms

EGT: Assuming N symbol averaging used in each phase setting, the bisection involves N complex multiplication (CM), $(N-1)$ real addition (RA), and a single real multiplication (RM) for signal energy estimation for each phase setting. Thus, for finding the maximum from these three such settings ($\beta_a, \beta_b,$ and β_c), CM, RA, and RM will be $3N, 3(N-1),$ and $3,$ respectively. Similarly, it can be shown that the early-late method involves $2N$ CM, $2(N-1)+1$ RA, and 1 RM for gradient estimate.

MRT: The MRT techniques incur more computational costs due to matrix computation and gradient vector estimation. For the LS-based technique, although (7) includes matrix inversion, the size of the matrix is 2×2 for $(\mathbf{W}\mathbf{W}^*)^{-1}$ and the inversion load is quite small. The remaining computation can be shown to have complexity of the order of N . This order of complexity also holds true for gradient vector estimation regarding the subspace-based and LMS-based techniques.

Thus, for a two-element array, the relative complexity counts for both the EGT and MRT techniques are on the order of the number of training or probing symbols. This implies that complexity count relies directly on convergence and, thus, convergence needs to be evaluated prior to comparing the relative complexity count among the proposed techniques. Convergence study has been addressed in detail in section IV.

Please note that a direct comparison or contrast with the existing TD techniques is not feasible due to the quite different nature of processing [1]-[4]; however, it is generally observed that the existing techniques rely heavily on matrix computation and elaborate optimization or search techniques while assuming perfect channel knowledge. Also note that the feasibility of feedback bandwidth is not always discussed. However, a good practical approach is given in [10] for the EGT type of implementation.

IV. Results

This section presents simulation results for performance comparison based on convergence and SNR improvement. Vector channels created from a channel simulator as well as indoor channel measurements were used to generate the results. The indoor channel measurements also address the effect of inter-element spacing on the performance of the proposed techniques. These studies are discussed in some details in the following subsections.

1. Convergence

A convergence criterion is defined in terms of number of symbols required to achieve performance within 5% or less of the optimal SNR value. The vector channel is assumed to

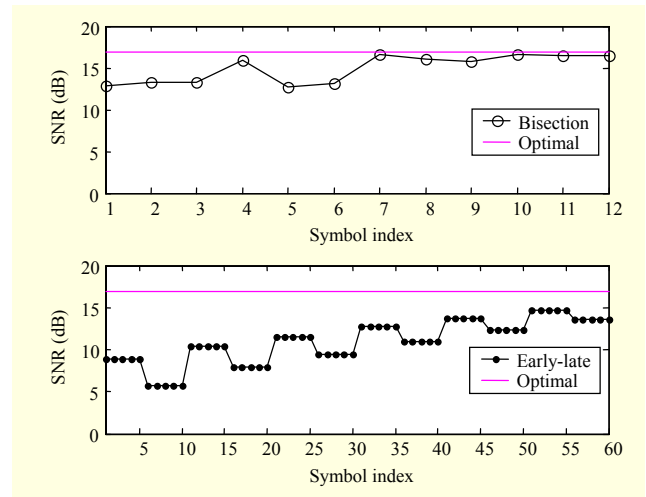


Fig. 3. Convergence plots for bisection method; early-late method ($\Delta\beta=15^\circ$ and $\mu=0.3$).

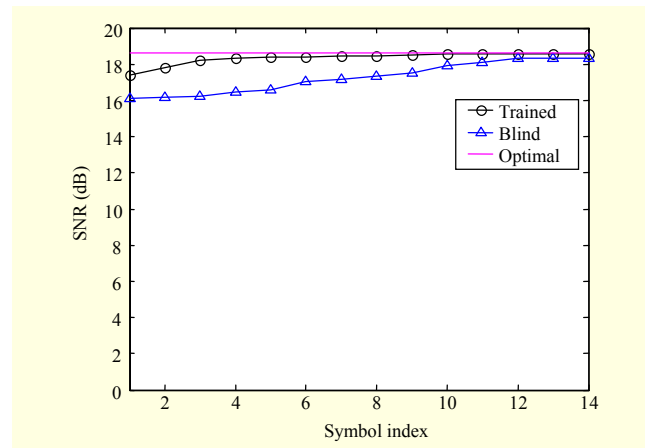


Fig. 4. Convergence plot for LS method.

follow independent and identically distributed (iid) Rayleigh fading distribution, and it is further assumed that the channel is stationary during the probing or estimation period (usually relevant for low mobility channels with large coherence time).

EGT: Figure 3 illustrates the variation of the combined SNR along with the optimal one provided by (3), with the number of symbols for the bisection and early-late methods at a fixed SNR of 15 dB in subplots 1 and 2, respectively. It can be seen that convergence is achieved within 9 to 12 iterations for the bisection method and in excess of sixty symbols for the early-late method, respectively. For the early-late method, step sizes of $\Delta\beta=15^\circ$ and $\mu=0.3$ have been used as this combination has been found to provide good performance. The stepped nature of the curve is due to the fact that there are several symbols associated with each SNR measurement for each setting.

MRT: Figure 4 shows convergence plots generated from an ensemble of snapshots using both the trained and blind mode of the LS technique for 15 dB SNR. The learning curves show

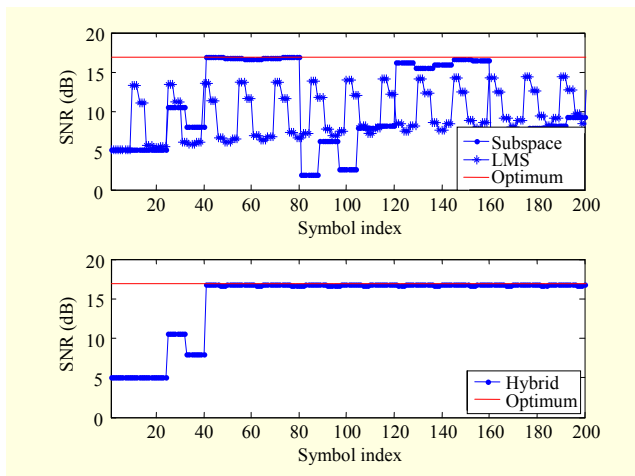


Fig. 5. Convergence plots for subspace method, LMS method, and hybrid method.

that the the LS techniques converge within 5 to 10 symbols for the trained mode and 15 to 20 symbols for the blind mode.

Figure 5 shows the convergence plots for the subspace, the LMS, and the hybrid methods. Each estimate of SNR for the subspace method is obtained from averaging over a period of eight symbols resulting in a step-like variation in the plot. The weight vector for the subspace method is updated at the end of every fifth step (considered as a single iteration). The algorithm achieves near-optimal performance from a single iteration involving about 40 symbols. The oscillatory behavior is due to the fact that the gradient estimate is accurate at locations in the cost function surface where it has a high value (that is, far from the optimal point), and it is degraded when it has a small value (that is, in the vicinity of the optimal point). Thus, approaching the optimal value, where the gradient is relatively flat, the next set of iterations yields a poor estimate of the weight vector. For the LMS method, the average of three symbols is used to estimate each derivative term. Here the trade-off is between convergence speed and output SNR variability. The amount of weight perturbation as well as the LMS step-size is chosen as relatively high for fast convergence. Even then, it needs more than 200 symbols until convergence is reached.

The convergence plot for the hybrid method is shown in the lower subplot of Fig. 5. The plot shows that by using the subspace method initially, the performance reaches close to the optimal point wherein the technique switches to the LMS to slowly approach that point. This approach offers a well-behaved SNR variation combined with a better convergence characteristic than that which is possible from either the subspace method or the LMS method alone.

2. Output SNR Improvement

Output SNR improvement in terms of diversity gain was

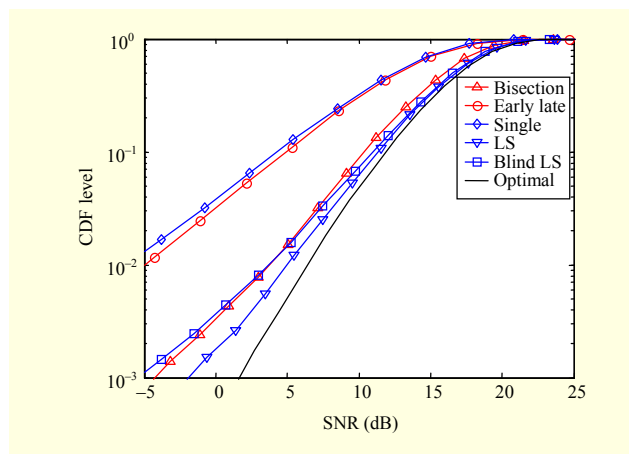


Fig. 6. Diversity gain from proposed transmit diversity techniques.

evaluated for quasi-stationary iid Rayleigh channels for an operating SNR of 20 dB. For each technique, the number of samples was chosen so that the technique attained convergence. Figure 6 shows the outage probability plots of the resulting output SNR. At the 1% outage level, all the proposed techniques (except for early-late) provide substantial gain, with the supervised LS (from MRT) and the bisection (from EGT) being better than the single antenna case by more than 10 dB and about 10 dB, respectively.

3. Practical Channel Measurements

Actual measured channels were used in the simulation to test the proposed techniques. Toward this end, vector channel measurements were performed in an indoor environment at a two-element array consisting of two quarter-wavelength dipoles with variable inter-element spacing, d , as shown in Fig. 7. The setup in Fig. 7 conforms to antenna array for a handheld device form-factor and addresses the effect of mutual coupling on the performance. Controlled measurements were performed by moving the array on a straight path of about two meters and collecting received signal samples at discrete intervals along the path. Based on channel reciprocity, the measured channels are assumed to hold true for a transmitter array with the same inter-element spacing (in fact, a separate experiment was performed to ensure that the channels were highly reciprocal). The experiments were repeated for different $d/\lambda \in \{0.1, 0.2, 0.3, 0.4, 0.5\}$ (λ for 2.05 GHz RF carrier frequency). Finite duration of sampled values of the fading profile were measured and used in the simulation study to compare the performance of different techniques. Two orientations of the array motion were realized: 1) inline orientation, where the array axis was along the direction of motion, and 2) broadside orientation, where the array axis was perpendicular to the direction of motion. A non-line-of-sight signal propagation was maintained between the transmitter and

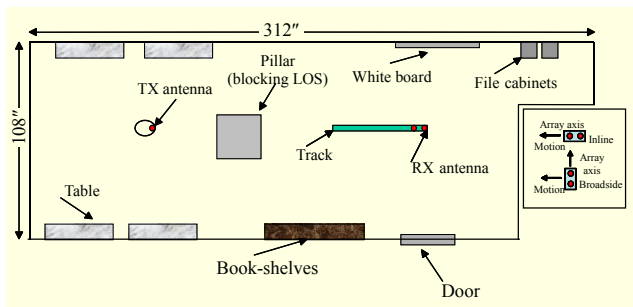


Fig. 7. Indoor environment for studying effect of antenna spacing on transmit diversity techniques.

the receiver.

The envelope cross-correlation coefficient between the individual fading channels at a particular inter-element spacing was computed as [32]

$$\rho_e = \frac{E[(e_i - \mu_i)(e_j - \mu_j)]}{\sqrt{E[(e_i - \mu_i)(e_i - \mu_i)^*]E[(e_j - \mu_j)(e_j - \mu_j)^*]}}, \quad (3)$$

where e_i and e_j are individual envelope measurements and μ_i and μ_j are the sample means of the respective envelopes.

The bisection from the EGT and the LS from MRT categories have been selected for performance evaluation with measured channels. The convergence behavior and the diversity gain have been considered in selecting these techniques from their respective categories. Table 1 shows the corresponding results. The single antenna case is represented by choosing the fading profile from one channel of the array.

Table 1(a) provides the computed gains in the inline orientation for different antenna element spacing. The results show that with increasing separation, the correlation coefficient decreases but the performance varies within small margins. The performance peaks at a spacing of 0.3λ and tapers off gradually in either direction of increasing/decreasing spacing. From Table 1(b), it is observed that the correlation values are relatively insensitive to inter-element spacing, and the performance for all the techniques improves with increasing separation. This transition is the most prominent going from $d/\lambda = 0.1$ to 0.2 and small for other changes. The effect of antenna separation on diversity performance for both the inline and broadside orientations can be explained in the context of pattern distortions that arise from closely spaced radiating elements. Radiation pattern measurements in the azimuth plane for two dipoles with $d/\lambda \in \{0.1, 0.3, 0.5\}$ are shown in Fig. 8 [22]. Here, the black dots represent antenna locations and the patterns correspond to the left element (marked by a black dot in the center). The patterns for the right element are assumed to be symmetrical, reflected across the center point of the array.

Both the measured and modeled plots show that the patterns

Table 1. Envelope cross-correlation and average output SNR in (a) inline orientation and (b) broadside orientation.

(a) Inline orientation						
d/λ	ρ_e	LS (trained) (dB)	LS (blind) (dB)	Bisection (dB)	Single ant. (dB)	Optimal (dB)
0.5	0.41	12.9	12.9	12.5	10.7	13.4
0.4	0.52	13.7	13.6	13.2	12.1	14.0
0.3	0.57	14.3	14.2	13.8	12.7	14.6
0.2	0.66	13.9	13.2	13.6	11.9	14.3
0.1	0.64	12.3	12.1	11.9	8.7	12.7
(b) Broadside orientation						
d/λ	ρ_e	LS (trained) (dB)	LS (blind) (dB)	Bisection (dB)	Single ant. (dB)	Optimal (dB)
0.5	0.17	11.5	11.3	10.7	7.8	12.0
0.4	0.18	10.3	9.4	9.5	6.5	10.9
0.3	0.14	10.3	10.0	9.7	6.5	10.9
0.2	0.01	10.0	9.7	9.2	5.5	10.6
0.1	0.16	7.9	6.9	7.4	4.2	8.7

become distorted and assume a directional shape instead of an omni-directional one. The directivity of the patterns is aligned with the axis of the array in most cases, and the maximum gain varies for different separations. The maximum gain for inline orientation occurs at a spacing of 0.3λ ($= 5$ dB, along the horizontal axis); for the other two spacings, the maximum gain is approximately the same (about 2.5 dB). In the broadside orientation, maximum gain occurs at a spacing of 0.5λ . These observations explain why the diversity gain is maximized at 0.3λ spacing for inline orientation and 0.5λ spacing for broadside orientation. Also, note that, for broadside orientation, the gain in the broadside direction increases from 0 dB to 2.5 dB when d/λ changes from 0.1 to 0.3, which explains the prominent increase in diversity performance. These results indicate that the proposed diversity techniques benefit from sufficient signal decorrelation at a tightly spaced array in indoor environments and render themselves feasible for small wireless devices.

Table 2 summarizes the key candidates from the EGT and MRT categories having relatively good convergence performance. The table shows that the LS (trained) method provides the best convergence, complexity, and diversity gain performance among the selected candidates.

4. Practical Implementation Issues

In this section, we conduct performance assessment under realistic propagation constraints that include a time varying channel gain profile, finite precision at the receiver, and the

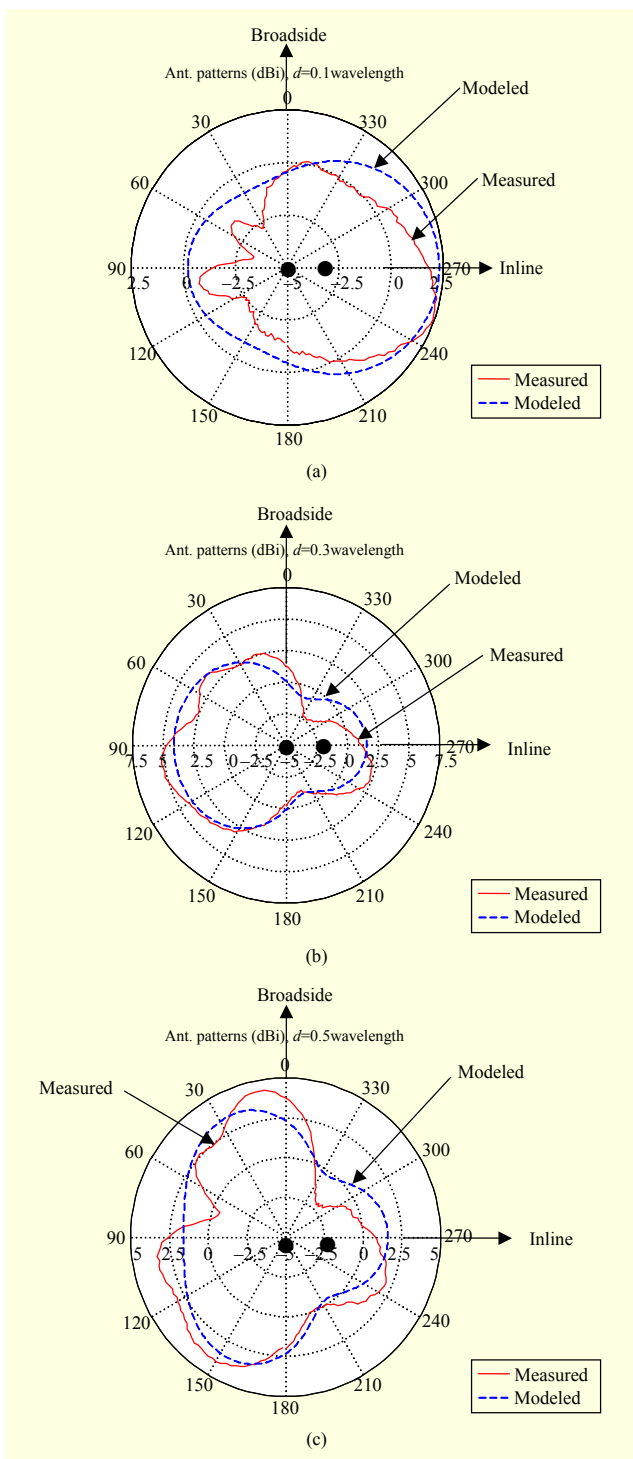


Fig. 8. Radiation pattern measurement plots for different interelement spacing; (a) $d=0.1\lambda$, (b) $d=0.3\lambda$, and (c) $d=0.5\lambda$ [22]; black dots represent antenna locations.

presence of feedback errors and delays (see Fig. 1). Among the proposed techniques, only the bisection from EGT and the LS from MRT have been selected for this study, based on their convergence and diversity gain performance. This pre-selection

Table 2. Summary of performance comparison.

Techniques	Iter # for convergence	Relative complexity count	Diversity gain at 1% outage	Measured output SNR gain at $d/\lambda=0.1$ (inline)
Bisection	9 to 12	Low	≈ 10 dB	11.9 dB
Early-late	60+	High	≈ 2 dB	N/A
LS (trained)	5 to 10	Low	≈ 12 dB	12.3 dB
LS (blind)	15 to 20	Moderate	≈ 10 dB	12.1 dB

is based on the assumption that in a practical operating scenario, only the best candidates from EGT and MRT will be considered for implementation in a handset.

The forward channel (from transmitter to receiver) is modeled with a fading envelope at certain mobility, whereas the feedback channel is characterized with a specific probability of error. In the remainder of this section, simulation results are presented to evaluate performance of some of the proposed techniques for the W-CDMA standard with reference to the model shown in Fig. 1. The overall latency, ΔL associated with a closed-loop application, uplink power control mechanism, is given in [7], and it can be inferred that the maximum ΔL comes out to be around 1-2 slots for practical cell radii. ΔL , in general, can be expressed as $\Delta L = (2\tau_p + \tau_1 + \tau_2)$, where τ_p is the propagation delay and τ_1, τ_2 are processing delays at the receiver and transmitter, respectively. In this study, latency values of 1 and 5 slots, representing both practical and pessimistic estimates, are used to test the proposed algorithms. Pedestrian speed is considered by assuming a velocity $V = 3$ mi/h, and fading channels are generated at the slot rate (1,500 Hz) using the Rayleigh fading channel simulator with the maximum Doppler corresponding to this velocity. The time coherence of the channel is assumed to span more than a slot at this low mobility. Two different feedback error rates $p_e \in \{0.01, 0.05\}$ were considered. The operating SNR is assumed to be 20 dB.

One iteration of the bisection technique follows a closed-loop path from the receiver through the channel to the transmitter array, and, thus, convergence characteristics and overall performance are subject to distortions arising from the practical constraints. On the other hand, the LS technique works in a block mode and thus is subject to distortions only once per probing process. The feedback information for the bisection method is an integer value $i \in \{1, 2, 3\}$ that can be quantized by two bits. For the LS technique, the feedback information is the estimated weight vector whose magnitude and phase information for each component can be quantized to a finite number of bits. The feedback payload in this investigation accommodates two bits for magnitude and three

Table 3. Performance from (a) LS (trained and blind) and (b) bisection with practical implementation constraints; $V = 3$ mi/h.

(a) LS (trained and blind)					
Latency ΔL	p_e	LS (blind) (dB)	LS (trained) (dB)	Single ant. (dB)	Ideal MRT (dB)
1	0.01	18.2	18.3	15.7	18.7
	0.05	17.6	17.7		
5	0.01	17.5	18.2		
	0.05	17.1	17.7		
(b) Bisection					
Latency ΔL	p_e	Bisection (dB)		Single ant. (dB)	Ideal MRT (dB)
1	0.01	15.7		13.7	16.7
	0.05	15.6			
5	0.01	15.2			
	0.05	15.2			

bits for phase for each component in the weight vector. Experiments were carried to test non-uniform quantization (based on the Lloyd-Max algorithm [29]) primarily by excluding other sources of distortions, and it was observed that quantization with 5 bits introduces a small degradation of around 0.1 dB compared to the infinite precision case. The results, expressed as the mean receive SNR in dB, are presented in Table 3.

From Table 3(a), it can be seen that both the versions of the LS method are relatively insensitive to practical channel conditions. The performance from the trained LS method is dominated by the error rate irrespective of latency, and the performance degradation from the ideal system is about 0.4 dB and 0.9 dB for p_e of 1% and 5%, respectively. The blind version of the LS method is adversely affected by both latency and feedback error rate; however, the range of performance degradation is relatively small, the highest being 1.5 dB occurring at the extreme setting of latency and error rate (that is, $\Delta L = 5$ and $p_e = 0.05$). Even at the extreme setting, both versions of the LS method provide substantial performance gain over the single antenna system. Please note that the results reported in these tables are average SNR outputs, and the related outage performance (more important for closing the link in any communication system) is expected to be more impressive.

It is evident from Table 3(b) that the bisection method is also relatively robust to practical channel constraints. The performance depends on both latency and error rate; however, the degradation is small at the extreme setting of these parameters. The bisection method still provides a gain of 1.5

dB over the single antenna system even at this setting. Note that a single iteration of the technique involves closed-loop feedback and the occurrence of errors along with latency can cause the algorithm to diverge to an incorrect solution. With $\Delta L = 5$, the length of the channel spanned by the algorithm may exceed the coherence time of the channel. However, results show that under reasonable operating constraints and in a low mobility environment with small propagation delay, the proposed techniques provide substantial performance improvement over single-antenna systems.

We note that the latency associated with indoor wireless channels is smaller than the latency considered in this paper [33]. Thus, indoor channels will provide a vantage scenario for the algorithms under consideration. For indoor-type applications, both the simulation results and measurements (under both ideal and practical channel constraints) in this paper weigh in favor of the implementation of these algorithms.

5. Comments on Cost/Benefits Comparison with Single Antenna Operation

It is worthwhile to compare the proposed techniques with the single antenna in terms of the cost-benefit factor. Similar to the previous sections, we will focus on the bisection and the LS methods for their superior performance over other techniques in their respective categories. It is evident from the results presented in the previous subsections that both of these techniques provide average SNR improvement over the single antenna case even in a practical operating condition including various error sources. In an indoor environment with pedestrian mobility and reasonable values of latency and propagation errors, these techniques offer an average SNR improvement on the order of 1.5 dB, implying that the outage improvement (that is, diversity gain) will be significant in such an operating scenario. However, there will be costs associated with implementing such techniques in a practical handset. For a two-element array system, this cost factor is expected to be minimal compared to the overall complexity of modern-day wireless devices and due to the miniaturization that is possible from such devices. Thus, the benefits that are possible from these techniques are expected to outweigh the associated costs of implementation in a small wireless terminal.

V. Conclusion

This paper proposed and evaluated several transmit diversity algorithms for application in small wireless terminals. The design philosophy focused on simplicity of operation to reduce processing burden and to provide rapid convergence to counter channel dynamics. Practical aspects such as the impact of inter-element spacing on the performance were studied through

experimentation. Channel dynamics and operating constraints related to closed-loop operation were addressed at pedestrian speed. Simulation results and channel measurements indicated the feasibility of the proposed techniques for small wireless terminal applications.

References

- [1] F. Rashid-Farrokhi, K.J.R. Liu, and L. Tassiulas, "Transmit Beamforming and Power Control for Cellular Wireless Systems," *IEEE J. Sel. Areas Commun.*, vol. 16, no. 8, Oct. 1998, pp. 1437-1449.
- [2] D. Gerlach and A. Paulraj, "Base Station Transmitting Antenna Arrays for Multipath Environments," *Signal Process.*, vol. 54, no. 1, Oct. 1996, pp. 59-73.
- [3] V.M. DaSilva and E.S. Sousa, "Fading-Resistant Transmission from Several Antennas," *Proc. IEEE Int. Symp. Personal Indoor Mobile Radio Commun.*, 1995, pp. 1218-1222.
- [4] P. Zetterberg and B. Ottersten, "The Spectrum Efficiency of a Base Station Antenna Array System for Spatially Selective Transmission," *Proc. IEEE 44th Veh. Technol. Conf.*, 1994, pp. 1517-1521.
- [5] T. Hwang and Y.(G.) Li, "Transmit Diversity for Down-Link MC-CDMA based on Energy Spreading Transform," *WCNC*, 2007, pp. 612-616.
- [6] K. Chang et al., "Open-Loop Transmit Diversity for Broadcast Channel Transmission in E-UTRA," *Proc. IEEE 66th Veh. Technol. Conf.*, 2007, pp. 1293-1297.
- [7] ETSI TS 125 214 "Physical Layer Procedures (FDD)," Mar. 2000.
- [8] N. Souto et al., "Transmit Diversity Schemes for High Speed Downlink Packet Access in 3.5G Cellular Systems," *Proc. 8th ISSSTA*, Sept. 2004, pp. 623-627.
- [9] J.W. Liang and A. Paulraj, "Forward Link Antenna Diversity Using Feedback for Indoor Communication Systems," *ICASSP*, 1995, pp. 1753-1755.
- [10] R.W. Heath and A. Paulraj, "A Simple Scheme for Transmit Diversity Using Partial Channel Feedback," *Proc. Conf. Record 32nd Asilomar Conf. Signals Syst. Computers*, vol. 2, 1998, pp. 1073-1077.
- [11] P. Ming-yu et al., "A Transmit Antenna Selection Diversity Scheme Based on ACK/NACK Feedback," *15th APCC*, 2009, pp. 24-27.
- [12] M.J. Fakhereddin, M. Sharif, and B. Hassibi, "Reduced Feedback and Random Beamforming for OFDM MIMO Broadcast Channels," *IEEE Trans. Commun.*, vol. 57, no. 12, Dec. 2009, pp. 3827-3835.
- [13] B. Raghothaman, G. Mandyam, and R.T. Derryberry, "Performance of Closed Loop Transmit Diversity with Feedback Delay," *Proc. 34th Asilomar Conf. Signals Syst. Computers*, vol. 1, 2000, pp. 102-105.
- [14] E.N. Onggosanusi et al., "Performance Analysis of Closed-Loop Transmit Diversity in the Presence of Feedback Delay," *IEEE Trans. Commun.*, vol. 49, Sept. 2001, pp. 1618-1630.
- [15] S.C. Ip et al., "A New Fast Sub-Optimal Search Method for Closed-Loop Transmit Diversity System with Limited Number of Feedback Bits," *Proc. IEEE RAWCON*, 2004, pp. 387-390.
- [16] K.C. Hwang and K.B. Lee, "Efficient Weight Vector Representation for Closed-Loop Transmit Diversity," *IEEE Trans. Commun.*, vol. 52, no. 1, Jan. 2004, pp. 9-16.
- [17] S. Parkvall et al., "Transmit Diversity in WCDMA: Link and System Level Results," *Proc. VTC*, 2000, pp. 864-868.
- [18] J. Hamalainen and R. Wichman, "Performance Analysis of Closed-Loop Transmit Diversity in the Presence of Feedback Errors," *Proc. IEEE PIMRC*, vol. 5, Sept. 2002, pp. 2297-2301.
- [19] A. Heidari and A.K. Khandani, "Closed-Loop Transmit Diversity with Imperfect Feedback," *IEEE Trans. Wireless Commun.*, vol. 9, no. 9, Sept. 2010, pp. 2737-2741.
- [20] J. Choi, "Performance Analysis for Transmit Antenna Diversity with/without Channel Information," *IEEE Trans. Veh. Technol.*, vol. 51, no. 1, Jan. 2002, pp. 101-113.
- [21] N.-S. Kim and Y.H. Lee, "Effect of Channel Estimation Errors and Feedback Delay on the Performance of Closed-Loop Transmit Diversity System," *Proc. IEEE Workshop SPAWC*, June 2003, pp. 542-545.
- [22] C.B. Dietrich et al., "Spatial, Polarization, and Pattern Diversity for Wireless Handheld Terminals," *IEEE Trans. Antennas Propag.*, vol. 49, no. 9, Sept. 2001, pp. 1271-1281.
- [23] Transmit Diversity Enabled Chipsets from Magnolia. Available: <http://magnoliabroadband.com/>
- [24] V.K.N. Lau, Y. Liu, and T.-A. Chen, "The Role of Transmit Diversity on Wireless Communications-Reverse Link Analysis with Partial Feedback," *IEEE Trans. Commun.*, vol. 50, Dec. 2002, pp. 2082-2090.
- [25] J.-H. Kim et al., "Reverse Link Capacity and Interference Statistics of DS/CDMA with Transmit Diversity," *Proc. IEEE 60th Veh. Technol. Conf.*, vol. 6, Sept. 2004, pp. 4320-4324.
- [26] R. Mostafa et al., "Demonstration of Real-Time Wideband Transmit Diversity at the Handset in an Indoor Wireless Channel," *Proc. VTC*, 2001, pp. 2072-2076.
- [27] Telmo André Rodrigues Batista, "Capacity Increase in UMTS/HSPA+ Through the Use of MIMO Systems," July 2008, MS Thesis submitted to Instituto Superior Tecnico, Universidade Tecnica de Lisboa.
- [28] "HSPA+ for Enhanced Mobile Broadband," Qualcomm Inc., Feb. 2009.
- [29] J.G. Proakis, *Digital Communications*, 3rd ed., New York: McGraw Hill, 1995.
- [30] T.K.Y. Lo, "Maximum Ratio Transmission," *IEEE Trans. Commun.*, vol. 47, no. 10, Oct. 1999, pp. 1458-1461.
- [31] G.H. Golub and C.F. Van Loan, *Matrix Computations*, 2nd ed.,

Baltimore: Johns Hopkins University Library Press, 1993.

- [32] B.M. Green and M.A. Jensen, "Diversity Performance of Dual-Antenna Handsets Near Operator Tissue," *IEEE Trans. Antennas Propag.*, vol. 48, no. 7, July 2000, pp. 1017-1024.
- [33] R. Prasad, *Universal Wireless Personal Communications*, Chapter 6, Boston: Artech House Publishers 1998.



Raqibul Mostafa received his BS in electrical and electronics engineering in 1991 from Bangladesh University of Engineering and Technology, Dhaka, Bangladesh. He worked as a lecturer in the Department of Electrical and Electronics Engineering of the same university for a year and a half before attending Virginia

Tech for graduate study. He obtained his MS and PhD degree in electrical engineering from Virginia Tech. He worked as a post-doctoral research faculty member in the MPRG Lab at Virginia Tech for a year. He joined the corporate research and development (CRD) division of Qualcomm Inc. in San Diego and worked on wireless communications standards and indoor communications projects. He is currently an associate professor in the EEE Department in the United International University (UIU) in Dhaka, Bangladesh.



Ramesh C. Pallat received his B.Tech in electronics and communication engineering from University of Calicut, Kerala, India, in 1998. He earned his MS and PhD in electrical engineering from Virginia Tech, Blacksburg, USA, in 2002 and 2006, respectively. He is a senior researcher at Nokia Research Center,

Berkeley, USA. He was a co-founder of Fawna Inc., developing a novel high capacity wireless network architecture. He was a staff engineer with Qualcomm Flarion Technologies from 2007 to 2010, where he worked on FlashLinQ, a novel peer-to-peer wireless network technology. He was a graduate research assistant at Wireless@VT until 2006. His research interests include digital signal processing for wireless communication and building proof of concept prototypes for emerging wireless technologies.

Uwe Ringel received his MS in electrical engineering from Virginia Tech, Blacksburg, USA, in 1999. In 2001, he received an MS from Dresden University of Technology, Dresden, Germany. In 2001, he joined Siemens AG in the healthcare sector. In recent years he headed the Siemens AG Xray R&D department in Shanghai, China. Today, he holds a management position with them in Erlangen, Germany.

Ashok A. Tikku received his PhD in electrical engineering from the University of California, Berkeley, USA, specializing in the areas of system identification and system control. Since then, he has worked on

problems in control theory and signal processing problems in wireless communication systems.



Jeffrey H. Reed is the Willis G. Worcester professor in the Bradley Department of Electrical and Computer Engineering at Virginia Tech, Blacksburg, USA. He currently serves as the director of Wireless@VT, one of the largest and most comprehensive university wireless research groups in the US, and is the

founding faculty member of the Ted and Karyn Hume Center for National Security and Technology. Since joining Virginia Tech in 1992, he has been PI or co-PI of approximately 100 projects covering areas such as software radio, cognitive radio, ultra wideband, and channel modeling. He is cofounder of CRT Wireless, a company that is developing cognitive radio techniques for commercial and military systems, and Power Fingerprinting, a company focused on embedded device security. He is a fellow of the IEEE for contributions to software radio and communications signal processing and for leadership in engineering education and is a past recipient of the College of Engineering Award for Excellence in Research. He is the author of three books and over 200 journal and conference papers. Dr. Reed has two new books scheduled for publication in 2012 in the areas of cellular communications and software defined and cognitive radio.